Energy, Mines and Resources Canada
Énergie, Mines et Ressources Canada

CANMET
Canada Centre for Mineral and Energy Technology
Centre canadien de la technologie des minéraux et de l'énergie

EXAMINATION OF CRACKED PLATES FROM THE HULL AND BILGE KEEL OF THE TANKER "IRVING ESKIMO"

R.D. MCDONALD AND J. HARBEC
WELDING AND
ENGINEERING & METAL PHYSICS SECTIONS

DECEMBER 1981

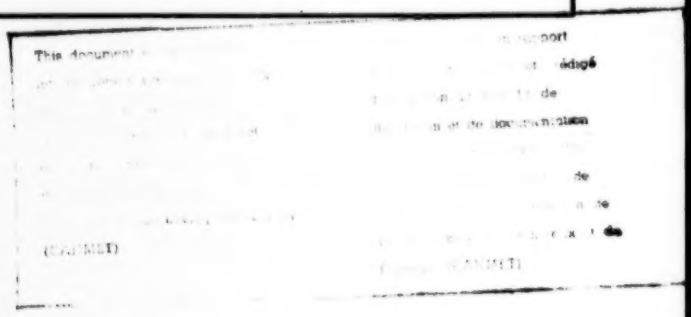

ENERGY RESEARCH PROGRAM

29 pp

PHYSICAL METALLURGY RESEARCH LABORATORIES
REPORT: ERP/PMRL 81-74(IR)

MICROMEDIA

PHYSICAL METALLURGY RESEARCH LABORATORIES
REPORT ERP/PMRL 81-74 (IR)

EXAMINATION OF CRACKED PLATES FROM THE HULL AND BILGE KEEL OF THE TANKER "IRVING ESKIMO"

by

R.D. McDonald and J. Harbec

ABSTRACT

After being in service for approximately eight months, the tanker "Irving Eskimo" developed a list while returning under ballast, to Saint John, New Brunswick, from Botwood, Newfoundland about March 18, 1981. The list was caused by a crack in the shell of the vessel. "Irving Eskimo" subsequently entered dry dock in Saint John for repairs. This investigation was carried out to determine fracture characteristics of sections of plate from the tanker, and the possible causes of failure.

It was evident that both fatigue and brittle fracture at about 2°C contributed to the failure. Brittle fracture initiated at a fillet weld joining the bilge-keel flat-bar to the hull and penetrated for a distance of about four metres into the hull plates. All flat-bar sections on the ship had fatigue failure at butt-welded joints from severe notches and cyclic stresses of undetermined origin. Stress concentrations in the region of the butt weld were enhanced by the design of the bilge-keel components.

Potential failures of this kind would be mitigated by reductions in the severity of cyclic stresses, improved bilge-keel design, and improved fracture toughness of steel plate used in hulls at the service temperatures encountered.

INTRODUCTION

The MV "Irving Eskimo", Fig. 1, is an oil tanker of about 35,000 tons, designed and constructed for service in ice. It was the second of four similar vessels to be built and it entered service in August, 1980. After being in service for eight months the vessel developed a list, while returning under ballast to St. John, New Brunswick, from Botwood, Newfoundland. The list was caused by a four-metre crack in the hull. The vessel entered dry dock in St. John for repairs.

During examination in dry dock, it was discovered that complete failure had occurred at the scalloped butt-welded juncture of all the bilge-keel flat-bars. In addition to the aforementioned damage, a severely deformed area was observed beneath the bow.

Transport Canada requested a metallurgical examination to assess the mechanical and metallurgical characteristics of the steel, to determine the origin of the cracks and to provide possible information on the mechanism of cracking.

This work was carried out as part of the CANMET Marine Materials Project which includes the evaluation of steel materials subjected to arctic service conditions.

Materials and Failure Description

Transport Canada arranged for shipment of cracked plate from the "Irving Eskimo" to CANMET for examination. A photographic record was made of the sections in their proper orientation, and of all pertinent fracture surfaces including those on flat-bars remote from the main fracture. The hull plate containing the fracture was flame cut for convenience and these sections are illustrated in Fig. 2 and shown in photographs Fig. 3 to 6. The main fracture occurred on the port side about 1/3 the way along the ship from the bow end. The crack extended vertically for about four metres almost equally above and below its apparent origin. The fracture appears to have originated at a fillet weld joining the bilge-keel flat-bar to the hull plate, Fig. 7. Arrest of the crack apparently occurred at the manual welds joining the upper bilge strake, N, to the top plate, M, and joining the lower bilge strake, Q, (source plate) to the bottom plate, S, Fig. 2. Views of the fracture at the upper and lower termination regions are shown in Figs. 8 and 9.

Several failed bilge-keel flat-bars, including the one adjacent to the main crack, Fig. 10, were provided for examination. All had failed at or near the butt welds joining the scalloped sections of flat-bars. Some examples remote from the main fracture are shown in Fig. 11.

PROCEDURE

Chemical Analysis

Sections 'C' in Fig. 2 were selected from each of the hull plates and from the adjacent flat bar for spectrochemical analyses.

Radiography

Radiographs were taken of the three welds where the main fractures intersected the welds and at the fillet weld adjacent to the apparent origin.

Fractographic Examination

The main fractures were examined visually at low magnifications, with scanning electron microscopy and with electron microscopy using the carbon replica technique (TEM). SEM and TEM examinations of the fractures at the origin, at the upper terminus of the main fracture and on the fatigue fracture of the flat bar nearest the origin were carried out.

Fracture mechanisms were characterized at these sites to assist in the assessment of causes of failure.

Mechanical Properties

Standard Charpy impact specimens were obtained from the top plate, M, the upper bilge strake, N, the source plate, Q, and the bottom plate, S, Fig. 2. In addition, longitudinal Charpy specimens were obtained within welds O, P and R to permit notching in the weld metal perpendicular to the plate. Charpy specimens were also obtained transverse to the weld, the notches being placed in the weld metal perpendicular to the plate surface.

Tensile properties were determined in the direction transverse to the main fracture, i.e., in the rolling direction of the plate. Standard 12.9 mm (0.505 in.) diam round specimens were obtained from 19.1 mm (3/4 in.) plates, N, Q, and S. Flat tensile specimens 12.7 mm x 12.7 mm (1/2 in. x 1/2 in.) gauge were obtained from the thinner 15.9 mm (5/8 in.) plate M.

Fatigue characteristics of welded joints in the bilge-keel were estimated by using the "proposed new Fatigue Design Rules For Steel Welded Joints in Offshore Structures".[1]

Metallographic Examination

Sections were removed from the apparent origin to permit a detailed examination of flat thumbnail-shaped areas at the toe of the fillet weld. These were referred to later as thumbnail-shaped "precracks", Fig. 7, arrow. An enlarged view of one of these areas was taken by SEM and is shown in Fig. 12. This area is located at the conjunction of the fillet-weld toe and the hull "source" plate Q. Two transverse sections, one near the extreme right and one near the middle, Fig. 12, were examined in detail metallographically.

In addition, sections were taken through welds at the upper and lower terminals of the main fracture for more detailed examinations.

Hardness surveys were conducted on weld zones.

RESULTS AND DISCUSSION

Chemical Analysis

The results of the analysis are shown in Table 1. All the steels can be classified as semi-killed and as satisfying the requirements of specification ASTM A131 Gr A., although plate N could be a fully killed steel because its silicon content is 0.20%. The top plate, M, containing 0.20% C and 1.0% Mn also complies with the chemical requirements of Gr B steel. All the plates exceed 12.7 mm (1/2 in.) in thickness and do not qualify as the exceptions shown in specification footnotes for thinner plates.

Radiography

Radiographs were taken at the origin of the fracture and near the locations where the submerged-arc automatic weld and the two manual welds intersected the main fracture.

Although minor defects were detected in the fillet weld near the apparent origin, they could not be directly associated with the initiation of the fracture. Lack of root penetration in an otherwise sound submerged-arc weld, P, appeared to be inconsequential in the progress of the main fracture.

The main fracture at its upper terminus passed through the manual weld between plates M and N, and stopped in the upper plate, M. At the lower

terminus the main fracture apparently stopped in the manual weld which joined plate Q (source plate) to the bottom plate. The crack turned toward the intersection of the horizontal and vertical welds, Fig. 6, and appeared to form several branches. The radiographic indications at the ends of the crack was verified by breaking open the plates after cooling them in liquid nitrogen. The results are illustrated in Figs. 8 and 9.

The upper part of brittle fracture arrested in the weld, Fig. 8, and extended by fatigue through the weld into the upper plate, M. The change in the mode of fracture to fatigue is marked on the lower section of the fractured plate by the smooth surface on the weld and the adjacent plate. The fracture ends at the light, freshly broken surface shown in the upper section.

The lower end of the brittle fracture was arrested fully in the lower manual weld, R, Figs. 2 and 9. Although smoothly contoured on the inboard side, R was very rough on the outer surface. The fracture showed evidence of branching and of changing direction at the tip and had partially penetrated into the vertical manual weld that was parallel to the main fracture. Although extensive porosity occurred in the outer passes of the horizontal manual weld near the juncture of the two welds, it had no apparent detrimental effect on the fracture.

Fractographic Examination

Main Fracture: Chevron markings along the major fracture surface were directed towards the apparent origin as shown in Figure 7. Examination of the fracture at its apparent origin with a low power optical microscope did not provide a conclusive assessment of the fracture characteristics. However, areas resembling cleavage were observed on the flat "precrack" regions at the toe of fillet welds at the origin, and on the main fracture surface.

Examinations of the precrack areas and the main fracture by SEM, Figs. 12 to 15, indicate that cleavage was the principal mode of fracture, although good definition was difficult because of corrosion modification of the fracture surfaces. There was no positive evidence of fatigue striations at the origin, although small regions of ductile fracture were associated with the cleavage fracture. These observations should be considered in the light of the effect of corrosive attack on the fracture characteristics. Furthermore, greater alteration of the precrack region by corrosion compared with the main fracture surface was believed to be an indication of the existence of the

precrack prior to the initiation of the main fracture. This evidence was supported by visual observation that the planes of the precrack regions did not coincide with the plane of the main fracture. Although all SEM observations are not included in the illustrations, those in Figs. 12 to 15 are representative of the several areas examined.

Examination of carbon replicas in the "precrack" area by transmission electron microscopy (TEM) confirmed that cleavage occurred over about 80% of the fracture, Fig. 16, the remainder being ductile as in Fig. 17. There was no positive evidence of fatigue, although modification of the surface by corrosive attack caused difficulty in ascertaining the original surface features.

Flat-Bars: Visual and low power microscopic examination of the bilge-keel flat-bar sections indicated that fatigue had initiated the fractures in all instances; the fractures usually originated at weld or flame cut edges where notches were prevalent. The direction of growth of the fractures was not consistent, they sometimes progressed toward the hull and sometimes away from it, Figs. 10 and 11.

The secondary fracture shown by the flat-bar in Fig. 10 was also examined by TEM to compare fracture characteristics in areas containing fatigue initiation sites, with fracture characteristics at the nearby origin, Figs. 16 and 17. Figure 18 shows that the flat-bar failed in a ductile fracture mode but there was no evidence of the striations that are sometimes apparent in fatigue fractographs. The ductile character of fatigue fracture was clearly distinguishable from the largely brittle character of the fracture at the origin.

Termini: Examination of the upper terminus of manual weld O by SEM, Fig. 2, is illustrated by Figs, 19 and 20. These fractographs show the region at the tip of the brittle area and the area identified as containing fatigue fracture. Despite some surface modification by corrosive processes, cleavage fracture is evident in the brittle region but not on the fatigued surface. This substantiated that the brittle fracture mode ended in the weld metal and fatigue then caused the crack to propagate through the remainder of the weld into the adjacent plate M.

Mechanical Properties

Tensile: The tensile properties of the plates received are shown in Table 2 with requirements of ASTM A131-80 for Grade A steel. The tensile

properties of all the plates except Q met the requirements of grade A steel. The yield strength of the source plate, Q, was lower than the specified value by 20 MPa.

Impact: The impact values obtained by standard Charpy tests are listed in Table 3(a) for plates M to S and in Table 3(b) for welds O, P, and R. All specimens were notched in the through thickness direction, i.e., normal to the plate surface. The specimens from the plate were oriented in the longitudinal direction with reference to the ship. This was the rolling direction of the plate.

The notches in all the specimens taken from welds were located in the weld metal normal to the plate surface. Longitudinal specimens were obtained parallel to the weld direction. Transverse specimens were obtained at right angles to the weld direction.

Although no energy requirement is made by specification ASTM A-131 for Grade A steel, it is assumed by IACS* that longitudinal Charpy impact energy in normal strength hull steel should be at least 27 J at 10°C[(2)]. A value of 27.2 J at 0°C is required for Grade B steel in thicknesses exceeding 25.4 mm. The steel in plate M (<25.4 mm) could qualify as Grade B steel from the results shown in Table 3(a).

Plate Q showed the least energy absorption of the four plates at 10°C and 20°C .

The impact energy absorption for weld metal shown in Table 3(b) was superior to the energy absorbed by all the plate steels at 0° to 2°C with the possible exception of plate M. The energy absorption for the upper manual weld was exceptionally high.

Fatigue: Fatigue tests were not conducted. However, stress estimates were calculated by taking into account the number of stress cycles the ship was exposed to during its eight months of service. It was estimated that the number of cycles (N) of wave motion during the period of service was approximately 6×10^5 and the number of cycles of engine vibration (propeller RPM) was 2.3×10^7. Using the Class E butt weld joint configuration shown in the "Appendix to Proposed new Fatigue Design Procedures" in BS Classification of Joints, (1) resulted in the following estimates:

---

*International Association of Classification Societies

(1) In air or cathodically protected in sea water -

Log (N) = 12.5169-1/3 log (5)

$N = 6 \times 10^5$ stress = 176 MPa (25 ksi)

$N = 2.3 \times 10^7$ stress = 52 MPa (8 ksi)

(2) Unprotected joints in sea water -

Log (N) = 12.5169-log 2 - 1/3 log (5)

$N = 6 \times 10^5$ stress = 140 MPa (20 ksi)

$N = 2.3 \times 10^7$ stress = 42 MPa (6 ksi)

Although the hull had been painted, the likelihood of paint damage would suggest that estimates based on unprotected joints in sea water would be the most appropriate for the Eskimo. These estimates further suggest that cyclic stress values as low as 41.5 MPa (6 ksi) might be expected to cause fatigue failure if these stresses are generated by vibrations at propeller frequencies.

Metallographic Examination

The metallographic examination was concentrated on the precracks at the toe of the fillet weld joining the flat-bar to plate Q in the region where the main fracture initated. The flat precrack or thumbnail-shaped area, Fig. 12, was examined on two planes normal to the precrack surface. A section was removed to permit an examination of the surface on the extreme right, Fig. 21, and a surface about midway along the precrack. These observations are shown in Figs. 22 to 24.

The microstructure in the transverse plane near the right corner of the precrack is snown at low magnification in Fig. 21. The short straight line evident in the upper left corner is the edge of the precrack that traverses the heat-affected zone (HAZ). The uppermost triangular-shaped configuration is a section of the weld metal and the light area at the bottom is the unaltered microstructure of the source plate, Q, with the jagged profile on the left representing a transverse view of the main fracture.

The microstructures contained dendritic ferrite in the as-cast weld deposits (Figs. 22 and 23) and a darker etched coarse-grained HAZ, adjacent to the weld metal, that becomes progressively finer toward the light etching hull plate, Q, Fig. 21. The coarse-grained ferritic matrix of the plate Q, Figs. 21 and 24, contains some pearlite and resembles an as-rolled microstructure.

A cold-worked region of weld metal and HAZ is apparent at the intersection of these regions, Figs. 21 and 22, and another cold-worked region is located at the step-like intersection of the HAZ with the plate steel in the upper left corner in Fig. 21. The transverse sections of the precrack, and the main fracture appear transgranular. A cold-worked region is apparent at the tip shown in the main fracture in plate Q, Fig. 21. All of the cold-worked regions probably occurred after the failure because of severe rubbing contact of the fracture surfaces.

No unusually hard zones were detected and spot hardness checks showed:

	DPN (conversion)	Rc
Weld metal -	264	25
HAZ -	246	22
Plate steel -	186	89 R_b.

The upper and lower termini of the main fracture were also examined metallographically. The manual weld at the upper terminus is shown lightly etched in Fig. 25. It shows a sound weld with multiple passes, most of which were applied from the outer surfaces to a depth of at least 2/3 the plate thickness.

The fracture at the lower terminus turned toward the intersection of the horizontal and vertical welds in a multi-branching manner. The fracture arrested in a very porous region of the lower horizontal weld shown in Fig. 9 and 26. There was no evidence that the porosity of the weld was detrimental, indeed it is possible that it contributed to a blunting effect on the crack tip in this instance.

Random hardness tests on the horizontal manual weld at the lower terminus provided hardness values below about 254 DPN (25 Rc) in all zones except for a small region near the root of the outer groove. In this region values from 301 to 675 DPN (30-59 Rc) were obtained. The microstructure associated with these hardnesses resembled those of a wear resistant iron. There was no evidence that this hard region was detrimental. However, the presence of an abnormal microstructure could indicate that a foreign material had somehow entered the weld metal.

GENERAL DISCUSSION

The investigation has shown that the "Irving Eskimo" had endured 6×10^5 cycles of wave motion and 2.3×10^7 cycles caused by propeller blades during its eight months of service according to design criteria on wave frequency and engine RPM. In this period all the butt welds in the flat-bars of the bilge-keel failed in a fatigue mode at the scallops. These fractures were random in their direction of propagation and initiated either at welds in the bilge-keel or at flame-cut edges of the plates. The four-metre vertical crack in the hull originated at the toe of the fillet weld in the flat-bar where the scalloped edge of the flat-bar joined the hull, Figs. 2 and 7. There was evidence in this instance that several brittle toe precracks occurred at the indicated origin and extended for 3 or 4 cm along the toe. The extensive length of the origin suggests a large region of high stress concentration at the toe of a poorly contoured fillet weld. A dynamic event, or possibly a high stress concentration, occurring at the extensive origin, after the bilge-keel flat-bar failed, initiated the brittle fracture in the hull plate without the necessity of additional fatigue penetration into the hull plate. This would be consistent with the absence of an extensive ductile transition zone between the precrack and the main brittle fracture in the hull plate. The lack of a substantial ductile zone is evidence of a small displacement type of failure that could only occur, under low strain rates, in a very brittle region.

The termination, or arrest of the main fracture, was possibly aided by the high energy absorptive capacity of the manual welds, Table 3(b). However, their complete effectiveness as "crack arrestors" over such a short distance is in question and other design features should be considered. The Charpy impact values of the weld metal in the manual welds at sea-water temperatures were far superior to those of the hull plate Q.

In summation, the problems leading to these failures begin with stress concentrations common to the bilge-keel design, that are exaggerated at welds joining the bilge-keel to the hull and welds joining the components of the bilge-keel.

The rapid fatigue failure of the bilge-keel flat-bars in relation to the service life of the ship indicates a high frequency of fatigue cycles more consistent with operating propeller vibration than with wave frequencies.

Stress estimates based on N the number of cycles to failure indicate that stresses at the higher frequency at welded joints need to be in excess of 41.5 MPa (6 ksi) to exceed the endurance limit for unprotected joints in sea water.

RECOMMENDATIONS

There should be two critical objectives in preventing serious failures in this type of ship. First, the reduction of fatigue cracking by reducing high cyclic stresses and stress concentrations in the bilge-keel and, second, the use of steel having high energy absorption capacity, at service temperatures, in critical regions. This two pronged approach should reduce fatigue cracking and, in the event cracking does occur, will permit repair before the cracks attain a critical size.

CONCLUSIONS

1. A large, vertical hull-crack originated at the weld toe of the bilge-keel scallop and progressed in a brittle mode for about four metres.
2. The cause of cracking was a combination of bilge-keel design, stress concentration at welds and fatigue failure at butt joints in the flat-bars.
3. The excessive flat-bar fatigue cracking during the relatively short life of the ship strongly indicates unusual high-frequency stresses not consistent with normal wave operational stresses.

REFERENCES

(1) H.W. Sneddon Offshore Installations; Guidance on Design and Construction. Proposed New Fatigue Design Rules For Steel Welded Joints in Offshore Structures. Marine Technology Support Unit, AERE Harwell Oxfordshire, Dept. of Energy, June 1981.

(2) Minutes of the Thirteenth Meeting of The International Association of Classification Societies (IACS) London 2nd-3rd June, 1980.

(3) The Canadian Shipbuilding and Ship Repairing Association Annual Report, 1980.

ACKNOWLEDGEMENTS

Assistance of the following persons in obtaining the information contained in this report is gratefully acknowledged - J. Ng-Yelim, V.P. Chartrand, K. Pickwick, R. Hoare, D.R. Munro, O. Vosikovsky, G.S. Weatherall, D. Lusk, and G.E. Palen.

Table 1. Chemical compositions of steel plate*

	Locations					ASTM A131 - 80 Grade	
	Plate M Top	Plate N upper bilge	Plate Q lower bilge	Plate S bottom	Flat bar	A	B
C	0.20	0.13	0.20	0.19	0.18	0.23 max	0.21 max
Mn	1.00	0.50	0.65	0.65	0.63	**	0.80-1.10
Si	0.015	0.20	0.023	0.028	0.03		0.35 max
S	0.025	0.027	0.040	0.032	0.028	0.05 max	0.04 max
P	0.010	0.020	0.007	0.005	0.007	0.05 max	0.04 max
Al	<0.005	<0.005	0.010	0.007	0.005		

*All plates exceed 12.7 mm thickness

**For all ordinary strength grades, the carbon content plus 1/6 of the manganese content shall not exceed 0.40%.

Table 2. Tensile properties

		Eskimo plates				ASTM A131-80
		M	N	Q	S	Grade A
UTS,	MPa**	466	415	424	398	400-490
YS,	MPa	278	248	216	244	235 min
El (50 mm)	%	35*	37	37	39	21% min 8 in.
RA	%					24% min 2 in.

*Elongation for flat specimen 50 mm gauge length. Tensile specimen was 12.7 mm x 12.7 mm at gauge. All others were standard 12.83 mm D at the gauge.

**1 ksi = 6.89 MPa

Table 3. Notch toughness by standard Charpy impact tests

(a)

PLATES

Absorbed Energy Joules*

Temperature	M		N		Q		S	
°C	Range	Average**	Range	Average	Range	Average	Range	Average
0	40-70	55	14- 62	33	11-13	12	20-26	24
10	64-78	69	67- 95	82	19-24	22	45-53	50
20	82-90	85	77-110	94	36-54	46	58-78	70
			Per cent shear fracture					
0	-	40	15-20	15	-	15	-	30
10	50-60	55	25-40	30	-	35	-	45
20	65-70	66	50-60	55	-	40	-	55

(b)

WELD METAL

Absorbed Energy Joules*

Temperature	O (Upper manual)		P (Sub-arc)		R (Lower manual)	
°C	Long.	Trans.	Long.	Trans.	Long.	Trans.
2	125	73	53	90	56	58
		Per cent shear fracture				
2	75	50	45	50	50	45

*Joules -- ft lb x 1.356

**Average of at least three specimens

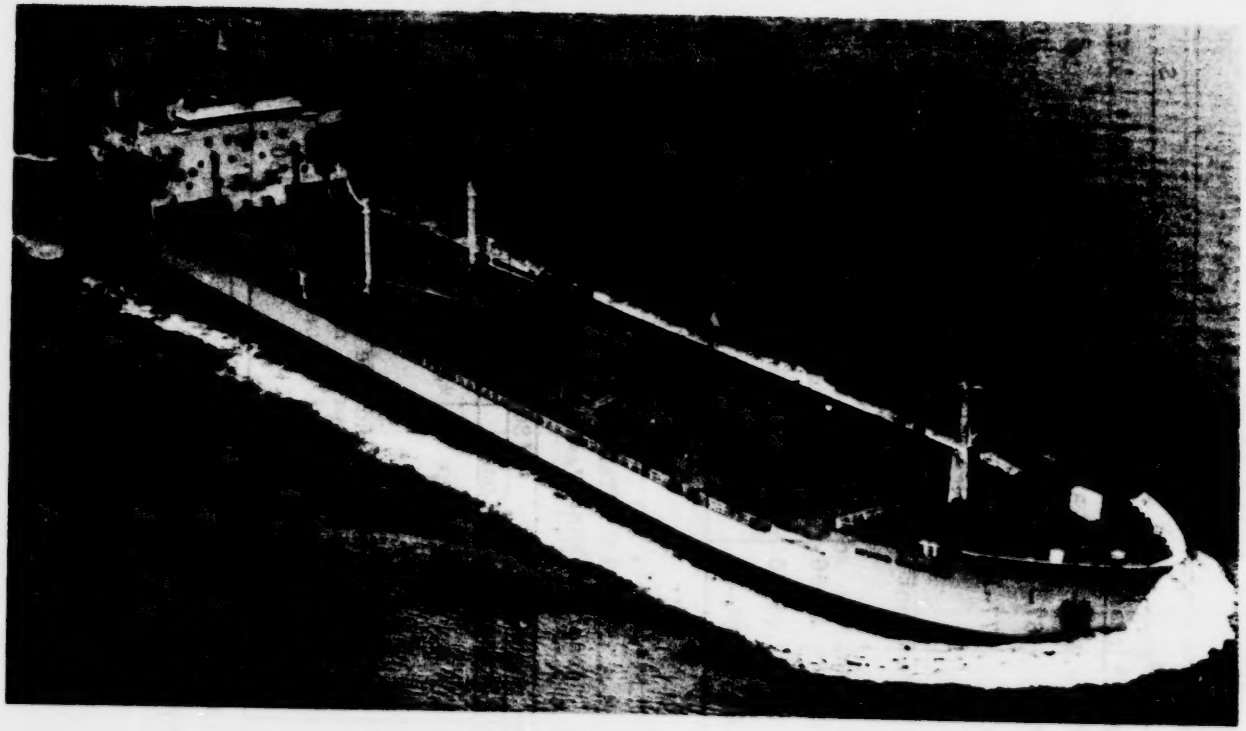

Fig. 1. "Irving Eskimo" is a 38,000 DWT Class Dirty/Clean Oil Carrier. The vessel is designed for world wide service and meets the Canadian Arctic Shipping Pollution Prevention Regulations for category B ships (3). (used with permission). (neg 5245)

SECTIONS OF FRACTURED PLATES FROM IRVING ESKIMO SHOWING LOCATIONS OF SPECIMENS

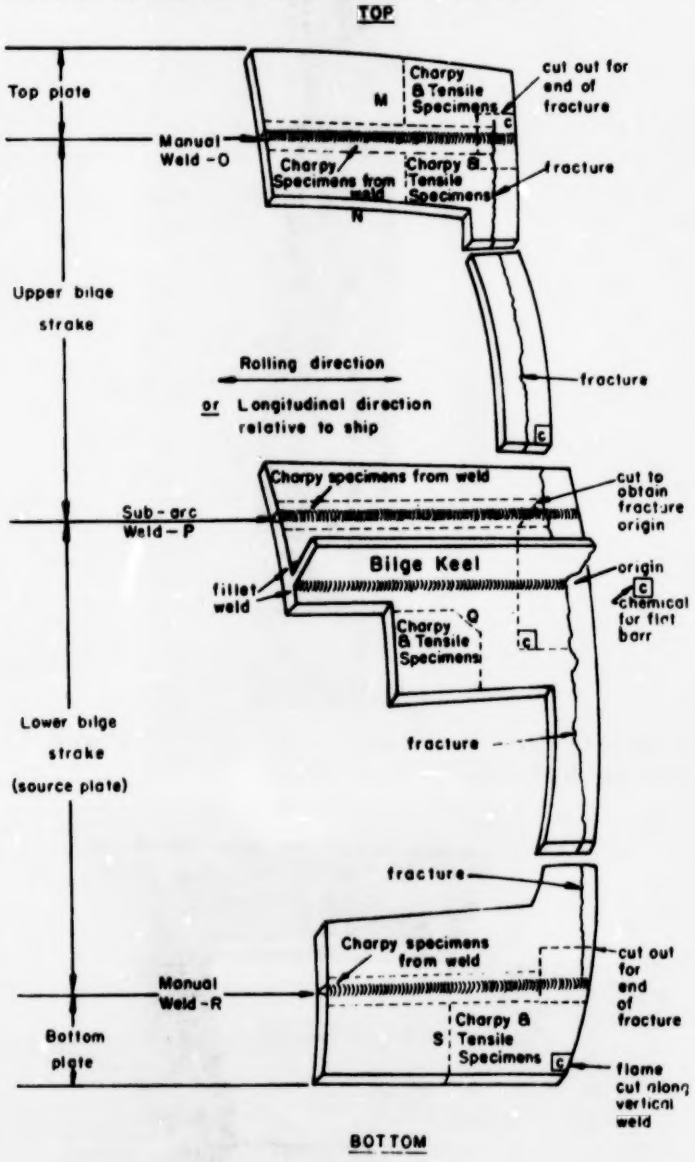

*C - Specimens for chemical analyses

Fig. 2. Illustration of sections of fractured plates from Irving Eskimo showing locations of specimens. (neg 6074)

Fig. 3. View of the fracture sections arranged in order from top to bottom. (neg 4585)

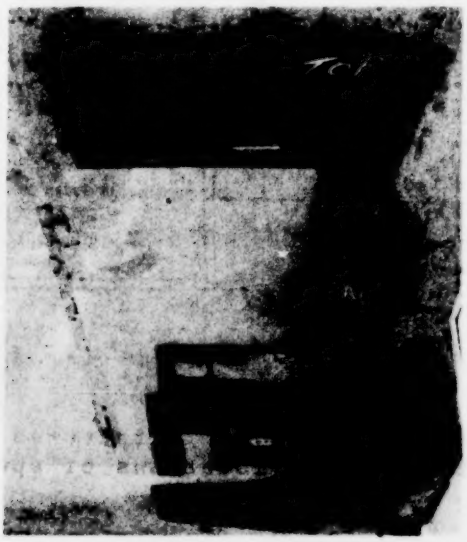

Fig. 4. Termination of the fracture at the top in a manual horizontal weld. (neg 4589)

Fig. 5. View of source plate, Q, containing the crack origin at the weld conjunction of the flat bar (5) with the hull. (neg 4584)

Fig. 6. Fracture termination at the bottom of source plate, Q, where the crack enters the manual weld, R, joining plates Q and S. (neg 4587)

Fig. 7. Brittle fracture origin at the toe joining the bilge-keel flat-bar to the hull (arrows indicate thumbnail-shaped precracks). (neg 4760)

Fig. 8. Enlarged view of the upper terminus of the fracture in the manual weld at plates M and N, showing the brittle zone in the weld (upper half as-received; lower half cleaned). (neg 4759)

Fig. 9. Termination of fracture in manual weld, R, joining plates Q and S (bottom of figure). (neg 5506)

Fig. 10. Fracture surface on aft section of flat-bars (5) near main origin showing secondary fatigue cracks with its origin circle. (neg 4750)

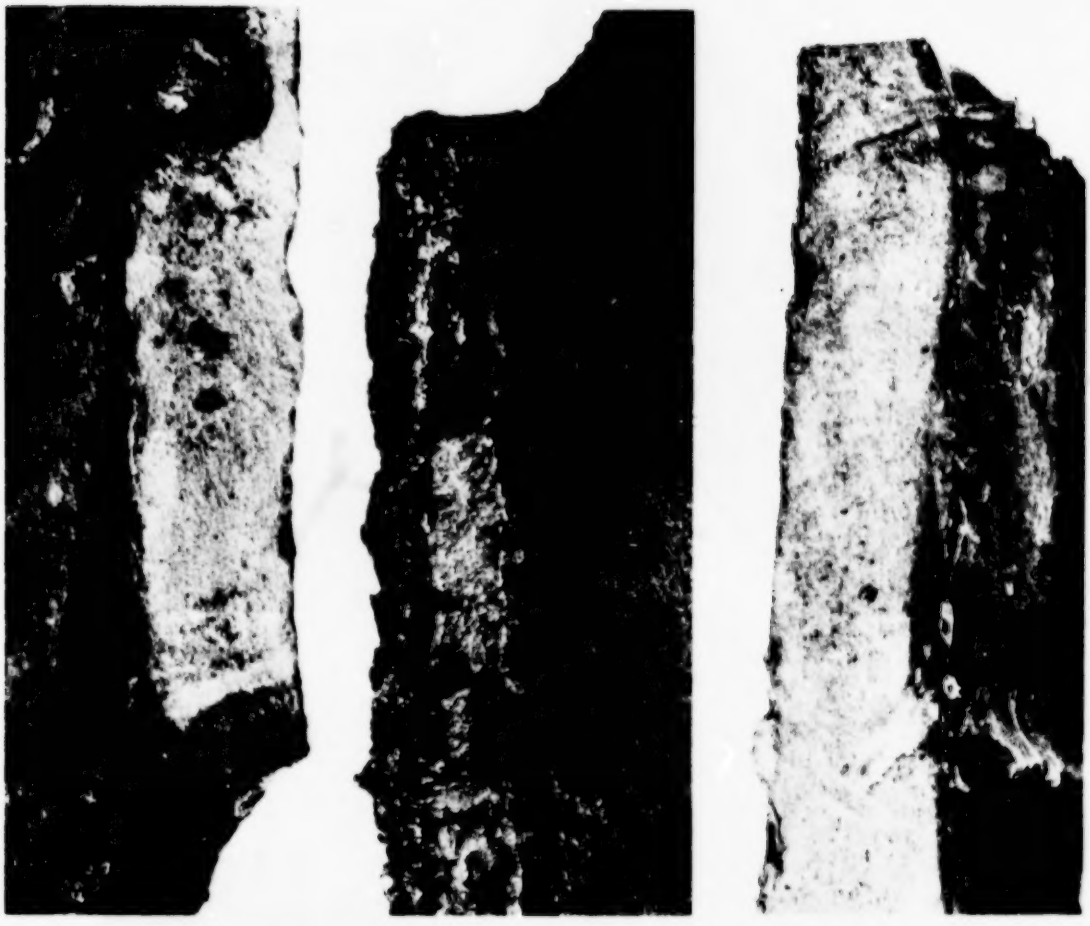

Port-forward
No. 1

Starboard
No. 5

Port forward
No. 6

Fig. 11. Examples of flat-bar fractures at other locations on the ship numbered as-received. X1 1/2. Initiation of fatigue apparently at flame-cut scallop, at the flat-bar butt weld, and at the bulb plate weld, with original direction of crack movement varied. (neg 4841)

Fig. 12. Composite of "thumbnail" shaped precrack associated with toe of fillet weld at origin of strain fracture (SEM). X15 (neg 5196)

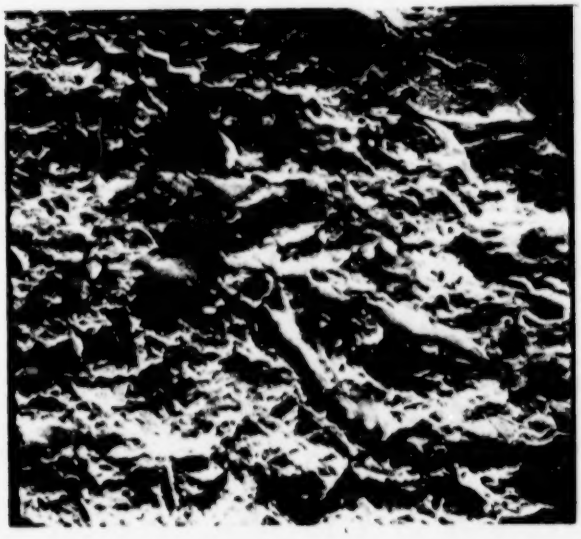

Fig. 13. View of precrack surface showing evidence of surface modification probably caused by corrosion (SEM). X200 (neg 6353)

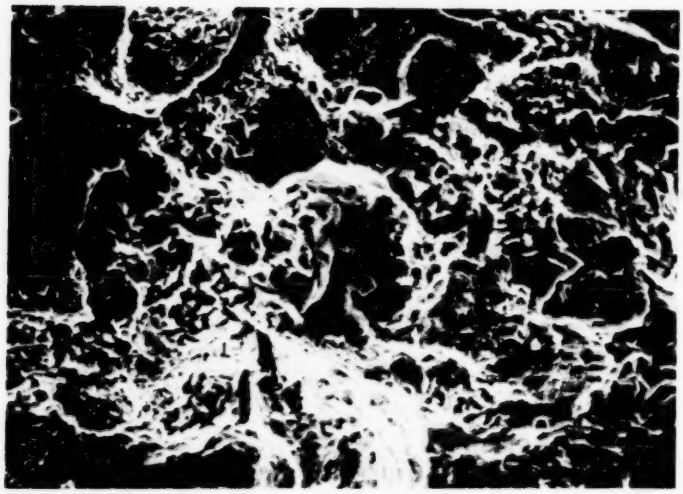

Fig. 14. Surface of precrack showing evidence of cleavage surfaces modified by corrosion attack (SEM). X1020. (neg 6072)

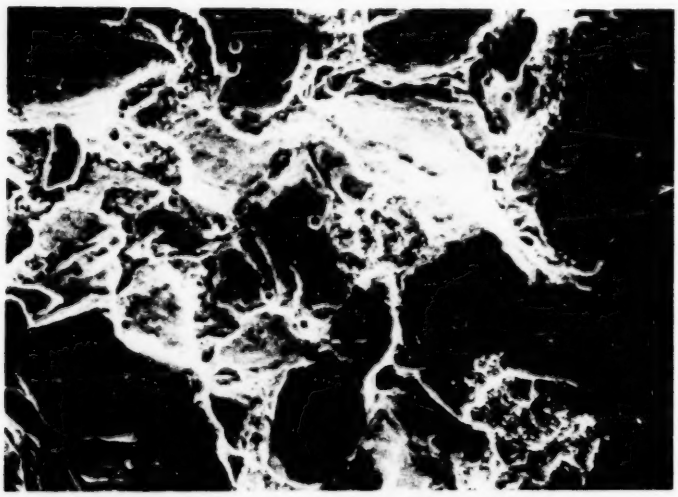

Fig. 15. Surface of main fracture showing cleavage facets indicative of brittle fracture (SEM) X1020. (neg. 6071)

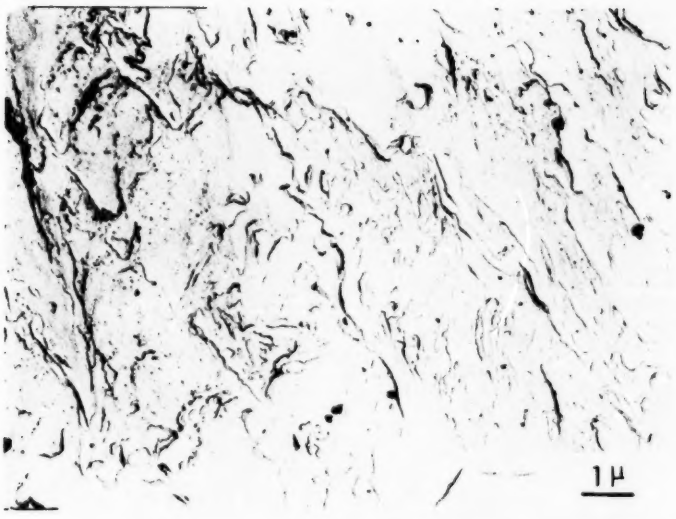

Fig. 16. Surface of precrack by transmission electron microscope, using carbon replica technique, showing corrosion modified cleavage facets representing about 80% of the area. (neg 6351)

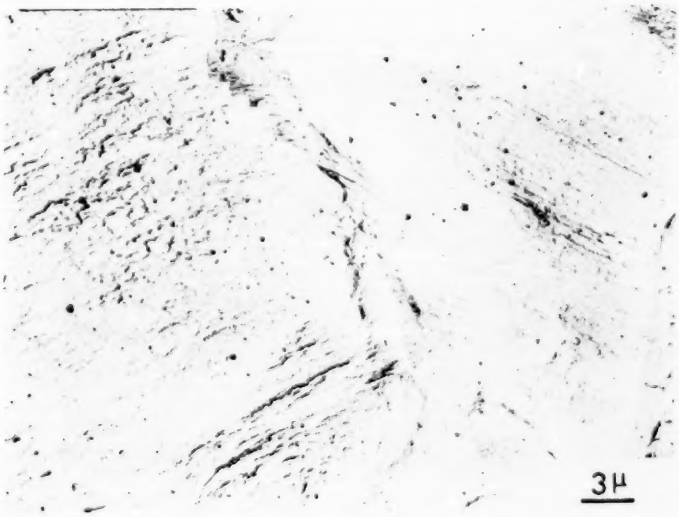

Fig. 17. Same general area as in Fig. 16 showing a view that represents about 20% of the fracture surface which appears ductile. (neg 6349)

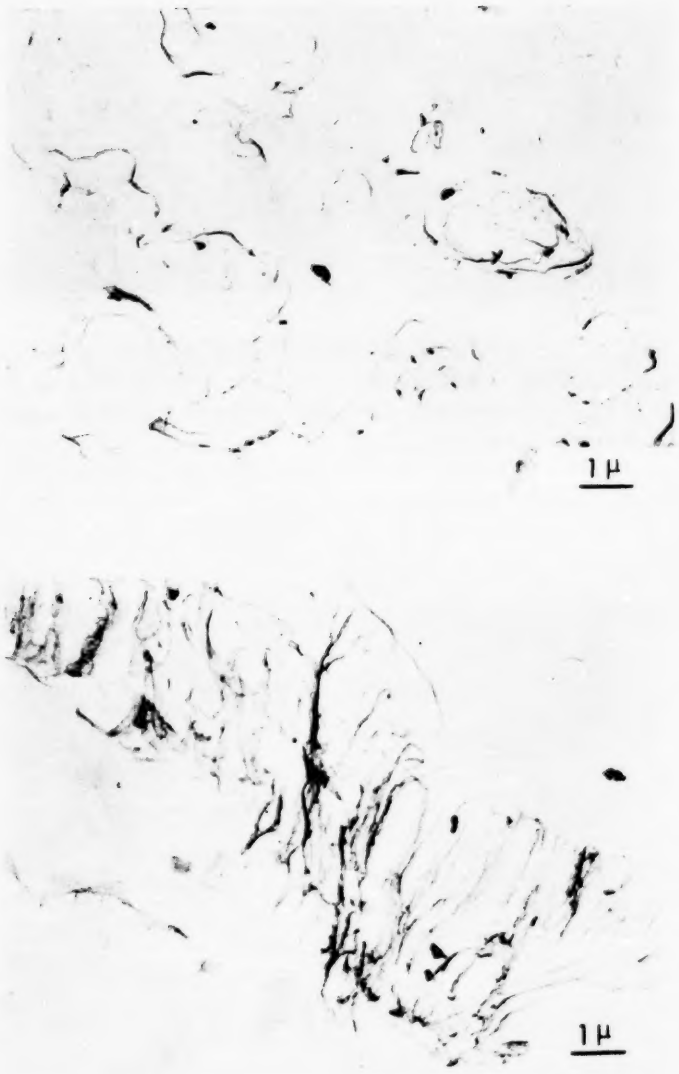

Fig. 18. View by transmission electron microscopy of fatigue on secondary fracture on flat bar adjacent to origin representing about 80% of the surface which failed in a ductile mode. (negs 6350 & 6352)

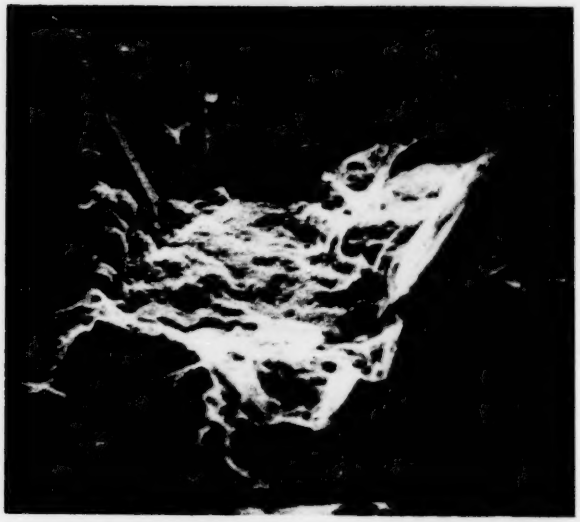

Fig. 19. Brittle fracture mode by SEM, plate N, showing evidence of cleavage in fracture. (neg 6347)

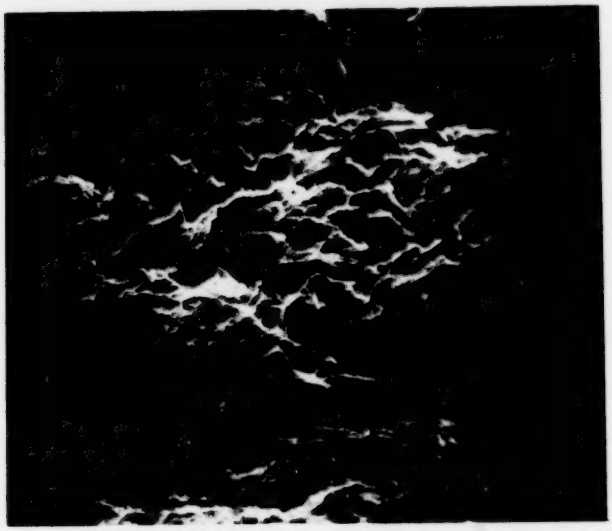

Fig. 20. Fatigue fracture mode by SEM, plate M, showing lack of cleavage. (neg 6348)

Fig. 21. View of cross section of "precrack" extreme right (Fig. 12). X7. (neg 6955)

Fig. 22. View of juncture of weld metal and coarse-grained heat-affected zone. X200. (neg 6953)

Fig. 23. Weld metal as in Fig. 21. X200. (neg 6954)

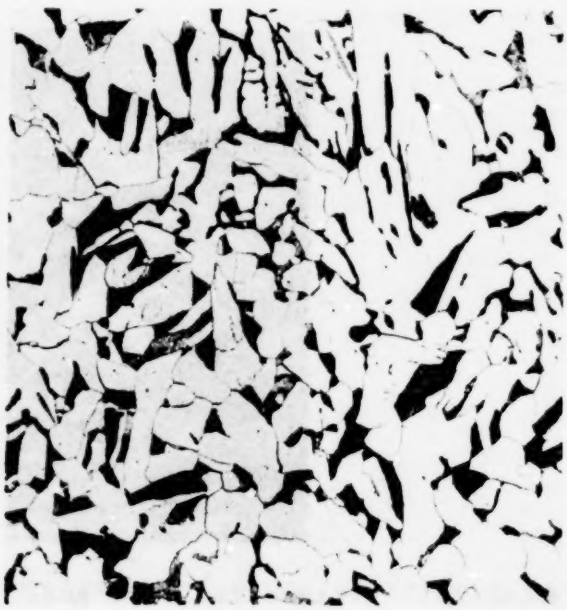

Fig. 24. Original microstructure of plate steel Q showing coarse ferritic grains. X200. (neg 6956)

Fig. 25. Weld in upper terminus of main fracture, Fig. 8, showing multiple passes. X1 1/2 approx. Etched in nital. (neg 5468)

Fig. 26. Weld at lower terminus of main fracture, Fig. 9, showing porosity associated mainly with outer weld. X2 approx. Etched in nital. (neg 6957)